Available online at www.sciencedirect.com
SCIENCE DIRECT
International Journal of Rock Mechanics & Mining Sciences 43 (2006) 847–859
International Journal of Rock Mechanics and Mining Sciences
www.elsevier.com/locate/ijrmms

System reliability approach to rock slope stability

R. Jimenez-Rodriguez[a,*], N. Sitar[b], J. Chacón[c]

[a]Department of Civil and Environmental Engineering, University of California at Berkeley, CA-94720-1710, USA Currently at ETS Ing. de Caminos, Canales y Puertos. Universidad Politécnica de Madrid, 28040, Spain
[b]Department of Civil and Environmental Engineering, University of California at Berkeley, CA-94720-1710, USA
[c]Departamento de Ingeniería Civil, Universidad de Granada, 18071, Spain

Accepted 30 November 2005
Available online 17 February 2006

Abstract

A systematic quantitative methodology for the reliability analysis of stability of rock slopes is presented. A sliding mass resting on an inclined plane and composed of two blocks separated by a vertical tension crack is considered, and a disjoint cut-set system formulation is proposed, with each cut-set corresponding to a different failure mode of the slope. Methods for the evaluation of the system reliability problem are discussed and applied to solve an example problem. Monte Carlo simulation method may be used to obtain the "exact" solution, at the expense of a higher computational cost, while methods based on first order approximations are found to be computationally efficient and to provide information of interest for the design process, but they are also shown not to be particularly accurate in some cases. The results also show that reliability bounds based on linear programming provide a flexible way of estimating the range of possible failure probabilities, and that accurate estimations of the probability of failure are obtained when sufficient information is considered.

Keywords: Probability; Risk; Monte Carlo; FORM; Linear programming

1. Introduction

In recent years, decision making, risk assessment and risk management procedures have become topics of increasing interest to researchers and practitioners working on rock engineering projects [1–3]. Hazard assessment and the quantification of the probability of occurrence of undesired events—i.e., failure probability—is a significant aspect of the problem of decision-making under uncertainty (see Fig. 1), and various methods have been applied to deal with uncertainty in rock slope stability problems. In general, these methods can be classified as methods that account for the uncertainty in the geometrical properties of the joint network (therefore having influence in the formation of removable blocks), and methods that consider uncertainties in the slope performance, with some attempts to achieve an integration between both [4].

Uncertainty in the geometrical characterization of fractures within the rock mass lead to the development of stochastic fracture network models. Dershowitz and Einstein [5] present a complete review of some of the more important stochastic models developed up to that time. New models have been developed since, with, for example, the inclusion of geological and mechanistic-based genetic considerations [6] and the development of fractal-based or geostatistical approaches [7–9]. Stochastic fracture network models have been used extensively to make predictions of formation of unstable blocks in rock slopes and underground excavations [10–15], and additional statistically based methods have been developed in order to estimate the parameters of fracture networks [16–21].

The other source of uncertainty which is usually dealt with in rock slope stability analyses is related to the probability of failure of the slope, given uncertain input parameters in the stability model. In rock slopes, methods of limit equilibrium analysis are usually employed, and they have been widely discussed in the literature [22–25].

*Corresponding author. Tel.: +34 91 336 6710; fax: +34 91 336 6774.
E-mail address: rjimenez@caminos.upm.es (R. Jimenez-Rodriguez).

1365-1609/$ - see front matter © 2006 Elsevier Ltd. All rights reserved.
doi:10.1016/j.ijrmms.2005.11.011

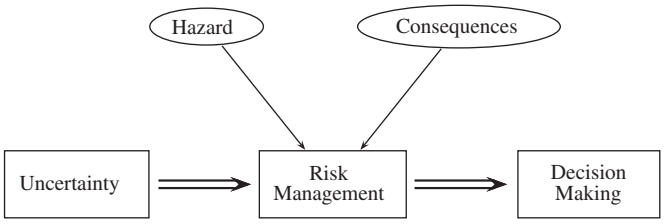

Fig. 1. The process of decision under uncertainty.

However, in order to estimate the influence that uncertainties have on the probability of failure, additional tools are needed beyond traditional analyses. Reliability-based approaches offer a very attractive framework for this task. Simulation methods, point-estimate methods and the first order-second moment (FOSM) method have been applied to slope stability problems [26–29], together with the first-order reliability method (FORM). For instance, Low presents a convenient implementation of FORM, based on the use of minimization tools readily available in spreadsheet software [30,31].

In this paper, we address the problem of system reliability analysis of rock slope stability. Our interest in methods to evaluate the reliability of general rock slope systems is motivated by the "rock engineering system" paradigm [32], which proposes that the complex performance of rock engineering designs is governed by the joint interaction of a number of different factors. System reliability techniques have been applied to the problem of slope stability before—usually in the context of a series system approach to the problem of slope failure along slip surfaces in soils [33,34]. More advanced tools are still needed, however, in order to perform reliability-based designs of rock slope systems. To that end, we present a general quantitative approach for solving the problem of system reliability analysis in rock engineering that provides a framework to support risk-based engineering decisions in a systematic and quantitative way.

2. Model formulation

For the purposes of illustration, we consider a simple sliding mass composed of two blocks separated by a vertical tension crack (see Fig. 2), resting on an inclined plane. The position of the tension crack and the water level in the crack are random. To simulate the effect of a buttress or rock reinforcement, a passive force T of uncertain magnitude is applied at the toe of the slope. For simplicity, the passive force is assumed to be normal to the plane of failure, as shown in Fig. 3.

In general, two sets of constraints must be fulfilled for a rock block to be potentially unstable:

- The first set of constraints—removability constraints [24]—refers to the kinematical admissibility of block displacements, which is influenced by the geometrical relations between the discontinuities forming the block and the excavation itself. Following the classical assumption of block theory [35], the orientation of the discontinuities forming the blocks is considered to be deterministic in this example. Hence, this condition is always fulfilled for the example considered herein.
- The second set of constraints refers to stability conditions of removable blocks under existing loads. Typically, the stability of removable blocks is assessed using limit equilibrium methods. Unstable removable blocks are referred to as *keyblocks* [24].

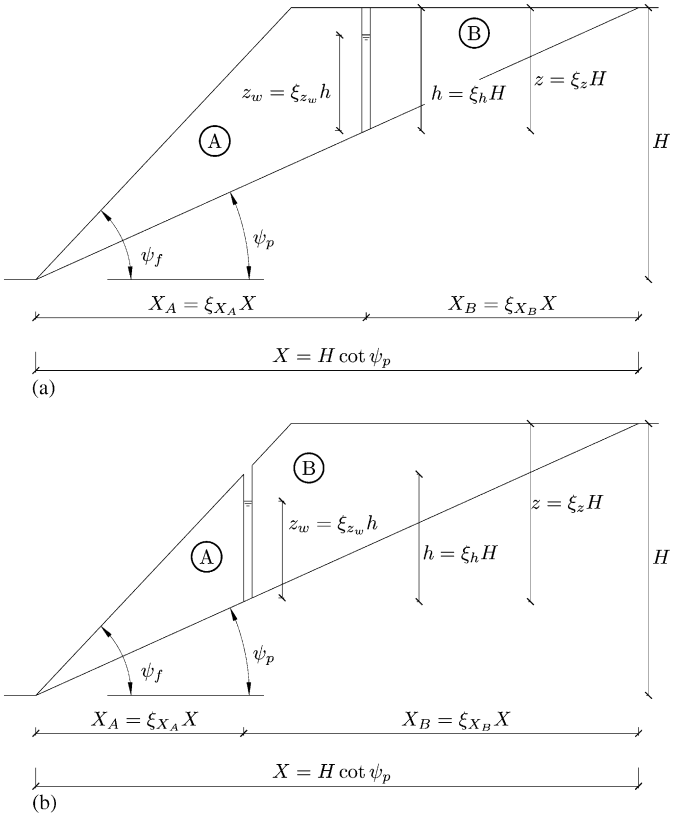

Fig. 2. Geometrical definitions of the considered slope stability model: (a) Tension crack at slope top; (b) tension crack at slope face.

In addition, we need to establish a clear distinction between success and failure events in order to perform a reliability analysis of the slope [36]. We will assume that the slope is safe when the factor of safety of block A is greater than unity ($FS_A > 1$), using the model presented by Hoek and Bray [22], with some modifications to consider the interaction between blocks.

Two different cases may be distinguished in the analysis, depending on the interaction between blocks A and B, as follows:

Case 1: Block B is stable by itself; i.e., there is no interaction between blocks.

Case 2: Block B is unstable; i.e., block B will tend to slide, imposing an interaction force, I_F, on block A.

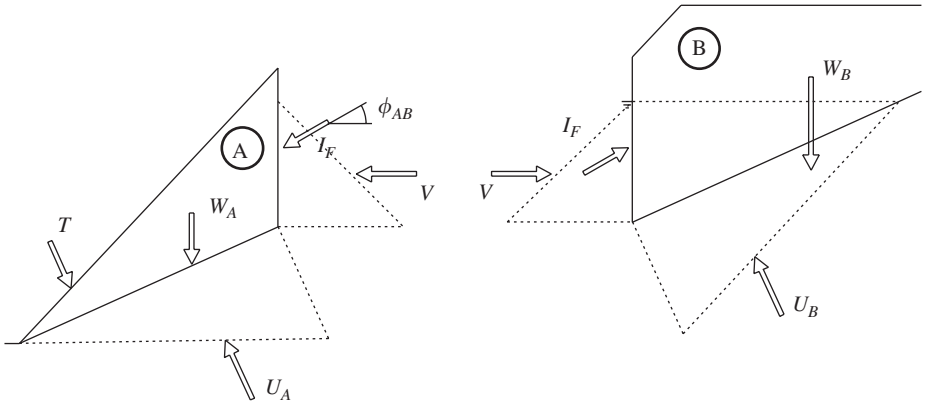

Fig. 3. Forces considered in the slope stability model.

2.1. Case 1: No interaction between blocks

In this case, we compute the factor of safety against sliding for block B, as [22]:

$$FS_B = \frac{c_B A_B + (W_B \cos\psi_p - U_B + V \sin\psi_p)\tan\phi_B}{W_B \sin\psi_p - V\cos\psi_p}, \quad (1)$$

where c_B is the cohesion along the failure surface and block B, ϕ_B is the friction angle, A_B is the area of contact with the failure surface, and U_B and V represent water pressure resultant forces. A_B, U_B and V are obtained as follows [22]:

$$A_B = z\csc\psi_p, \quad (2)$$

$$U_B = \tfrac{1}{2}\gamma_w z_w^2 \csc\psi_p, \quad (3)$$

$$V = \tfrac{1}{2}\gamma_w z_w^2. \quad (4)$$

W_B is the weight of block B. Depending on the location of the tension crack, we have:

- For the tension crack located at the top of the slope (see Fig. 2a):

$$W_B = \tfrac{1}{2}\gamma_{rock} z^2 \cot\psi_p, \quad (5)$$

- For the tension crack located at the slope face (see Fig. 2b):

$$W_B = \tfrac{1}{2}\gamma_{rock} H^2[\cot\psi_p(1-(1-z/H)^2 \times(\cot\psi_p\tan\psi_f - 1)) - \cot\psi_f]. \quad (6)$$

The transition between both cases will occur when the tension crack is located at the crest of the slope, that is when [22]:

$$z/H = (1 - \cot\psi_f \tan\psi_p). \quad (7)$$

Similarly, assuming that block B is stable, the factor of safety of block A is computed as [22]:

$$FS_A = \frac{c_A A_A + (T + W_A\cos\psi_p - U_A - V\sin\psi_p)\tan\phi_A}{W_A\sin\psi_p + V\cos\psi_p}, \quad (8)$$

where c_A, ϕ_A, U_A, and V have equivalent meanings as in Eq. (1), and T is the passive force applied at the toe of the slope. A_A and U_A are obtained by [22]:

$$A_A = (H - z)\csc\psi_p, \quad (9)$$

$$U_A = \tfrac{1}{2}\gamma_w z_w (H - z)\csc\psi_p, \quad (10)$$

and V is obtained by Eq. (4).

Again, the expression for the weight of block A will be different depending on the location of the tension crack [22]:

- For the tension crack located at the top of the slope:

$$W_A = \tfrac{1}{2}\gamma_{rock} H^2[(1-(z/H)^2)\cot\psi_p - \cot\psi_f], \quad (11)$$

- For the tension crack located at the slope face:

$$W_A = \tfrac{1}{2}\gamma_{rock} H^2[(1-z/H)^2\cot\psi_p(\cot\psi_p\tan\psi_f - 1)]. \quad (12)$$

2.2. Case 2: Interaction between blocks

This case occurs when block B is unstable by itself (i.e., $FS_B < 1$ in Eq. (1)), and tends to slide. One possible outcome is that block A is stable under the extra load due to block B (hence making block B stable), in which case the slope is considered to be stable. The other outcome is that block A is unstable, in which case failure occurs. The expressions of the factors of safety corresponding to blocks A and B will be similar to those presented in Eqs. (1) and (8), with the only modification that terms representing the interaction force, I_F, between both blocks need to be considered. Friction along the tension crack (of value ϕ_{AB})

is considered, and it is assumed that I_F has a direction inclined at an angle ϕ_{AB} with respect to the surface of the tension crack (see Fig. 3).

Maintaining the notation used in Section 2.1, the factors of safety of blocks A and B may be computed as:

$$FS_B = \frac{c_B A_B + [W_B \cos\psi_p - U_B + V \sin\psi_p + I_F \sin(\psi_p - \phi_{AB})]\tan\phi_B}{W_B \sin\psi_p - V \cos\psi_p - I_F \cos(\psi_p - \phi_{AB})}, \quad (13)$$

$$FS_A = \frac{c_A A_A + [T + W_A \cos\psi_p - U_A - V \sin\psi_p - I_F \sin(\psi_p - \phi_{AB})]\tan\phi_A}{W_A \sin\psi_p + V \cos\psi_p + I_F \cos(\psi_p - \phi_{AB})}, \quad (14)$$

where A, U, V, and W are given in Eqs. (2) to (12). Then, we can compute the value of I_F that makes $FS_B = 1$ in Eq. (13), and we can substitute it back into Eq. (14); the slope is considered to be stable if $FS_A > 1$, being unstable otherwise. The computed value of FS_A is not the "exact" value of the factor of safety for cases in which $FS_A \neq 1$. However, this approach provides us with the same failure domain as the "exact" solution, and hence provides the same reliability results.

3. Reliability analysis: General system formulation

We consider a system as an assembly of components, such that the state of the system is *uniquely defined* in terms of the states of its components. Without loss of generality, we additionally assume that for a system with N_g distinct components, each component i, has two possible states—e.g., failure (E_i) or safe ($\bar{E}_i$) state.

Several types of systems may be defined [38,39]. To make our approach systematic and comprehensive, we work with a *disjoint cut-set* formulation, in which the general system is represented by a series of N_{CS} parallel sub-systems, or cut-sets, C_k; such cut-sets are defined to be disjoint, that is $C_k \cap C_l = \emptyset$, for $k \neq l$ and $k, l = 1, \ldots, N_{CS}$. This allows a considerable simplification of the computations, since the probability of failure of the system may be obtained as the sum of the individual probabilities of failure of each cut-set (parallel sub-system), as follows:

$$P(E_{general}) = P\left(\bigcup_{k=1}^{N_{CS}} \bigcap_{i \in C_k} E_i\right) = \sum_{k=1}^{N_{CS}} P\left(\bigcap_{i \in C_k} E_i\right). \quad (15)$$

The performance of each component is defined by a *limit-state function* (LSF), so that component i is assumed to fail when its LSF is $g_i(\mathbf{x}) \leqslant 0$, and it is assumed to be in a safe state when $g_i(\mathbf{x}) > 0$. Fig. 4 shows the disjoint cut-set formulation for the slope stability model presented in Fig. 2. That is, the reliability problem is simplified to the evaluation of the probabilities of failure of $N_{CS} = 4$ disjoint cut-sets, with a total of $N_g = 7$ components. (Table 1 lists the physical interpretation of each LSF in the system.) Furthermore, each parallel sub-system in Fig. 4 may be associated with a mode of failure of the slope, as follows:

Failure mode 1: The tension crack is located at the top of the slope. *No interaction* between blocks *occurs*.

Failure mode 2: The tension crack is located at the top of the slope. *Interaction* between blocks *does occur*.

Failure mode 3: The tension crack is located at the face of the slope. *No interaction* between blocks *occurs*.

Failure mode 4: The tension crack is located at the face of the slope. *Interaction* between blocks *does occur*.

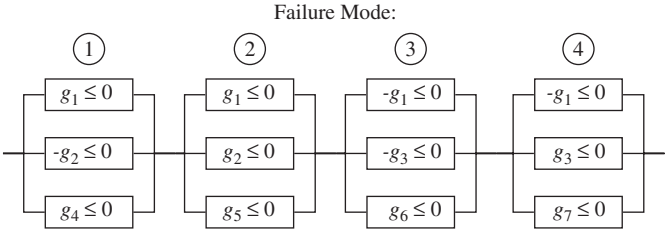

Fig. 4. Disjoint cut-sets system formulation of plane rock slide stability problem.

Table 1
Physical interpretation of limit state functions defining component performance in the system modeling the stability of the rock slope

Limit state function	Physical interpretation	Eqs.
$g_1 \equiv z - H(1 - \cot\psi_f \tan\psi_p) \leqslant 0$	Tension crack at top of slope	(7)
$g_2 \equiv \{FS_B \mid (g_1 \leqslant 0)\} - 1 \leqslant 0$	Block B is unstable (without interaction from A), given tension crack located at top of slope	(1), (5)
$g_3 \equiv \{FS_B \mid (g_1 > 0)\} - 1 \leqslant 0$	Block B is unstable (without interaction from A), given tension crack located at face of slope	(1), (6)
$g_4 \equiv \{FS_A \mid (g_1 \leqslant 0, g_2 > 0)\} - 1 \leqslant 0$	Block A is unstable, given tension crack at top of slope and block B stable (no interaction occurs)	(8), (11)
$g_5 \equiv \{FS_A \mid (g_1 \leqslant 0, g_2 \leqslant 0)\} - 1 \leqslant 0$	Block A is unstable, given tension crack at top of slope and block B not stable (interaction occurs)	(14),(11)
$g_6 \equiv \{FS_A \mid (g_1 > 0, g_3 > 0)\} - 1 \leqslant 0$	Block A is unstable, given tension crack at face of slope and block B stable (no interaction occurs)	(8), (12)
$g_7 \equiv \{FS_A \mid (g_1 > 0, g_3 \leqslant 0)\} - 1 \leqslant 0$	Block A is unstable, given tension crack at face of slope and block B not stable (interaction occurs)	(14), (12)

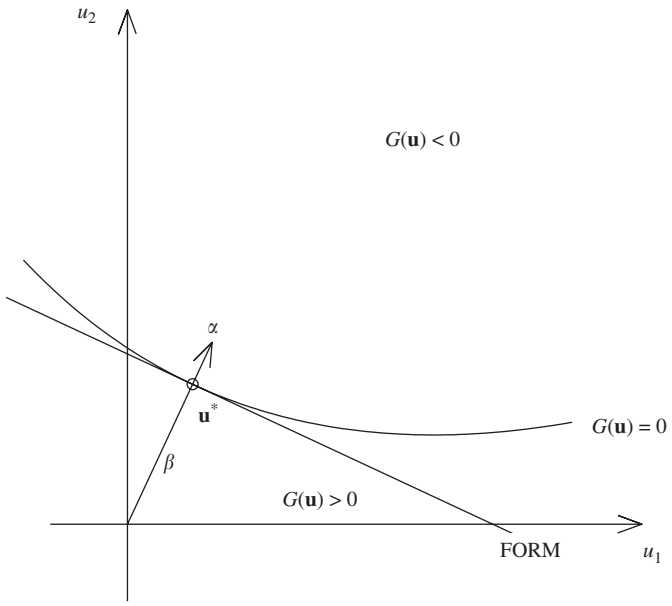

Fig. 5. FORM approximation to the failure surface in a two-dimensional standard normal space.

3.1. Component reliability

In order to compute the reliability of each parallel subsystem in the disjoint cut-set model, we start with the computation of the reliability of individual components. The probability of failure of a component is computed as:

$$P_f = P(g(\mathbf{x}) \leqslant 0) = \int_{g(\mathbf{x}) \leqslant 0} f(\mathbf{x})\, d\mathbf{x}, \tag{16}$$

where $f(\mathbf{x})$ is the joint probability density function (PDF) of the input variables $\mathbf{x}$ in the corresponding limit state function, $g(\mathbf{x})$. The *generalized reliability index* [40], is commonly used as an alternative measure of safety. It is defined as:

$$\beta_g = \Phi^{-1}(1 - P_f), \tag{17}$$

where $\Phi(\cdot)$ represents the *cumulative density function* (CDF) of the standard normal distribution.

The direct computation of integrals of the form of Eq. (16) is a complex and computationally intensive problem when standard methods of integration are used and a number of more efficient methods have been developed for such task. Among them, analytical methods, such as the first order reliability method (FORM), have found great acceptance. In general, FORM involves the following steps (see Fig. 5) [41]:

1. Transformation of the vector $\mathbf{x}$ of variables in the original space, into a vector of standard and uncorrelated normal variables $\mathbf{u}$ (the so-called standard normal space). This transformation produces a transformed limit state function, from the original $g(\mathbf{x}) \leqslant 0$ to the transformed $G(\mathbf{u}) \leqslant 0$. Details of the different transformations available—that can consider a general case, with non-gaussian and correlated random variables—are presented elsewhere [42,43].
2. Determination of the *design point* (i.e., the most likely failure point) in the standard normal space, $\mathbf{u}^*$. In order to obtain the design point, we must solve the following constraint minimization problem [44,45]:

$$\mathbf{u}^* = \min\{\|\mathbf{u}\| \mid G(\mathbf{u}) = 0\}. \tag{18}$$

   We use the *improved Hasofer Lind–Rackwitz Fiessler* (iHL–RF) algorithm [46], since it assures the convergence to a solution of (18).
3. The limit state surface in the standard normal space is approximated with the corresponding first order approximation at the design point:

$$G(\mathbf{u}) \approx \nabla G^{\mathrm{T}}_{|\mathbf{u}^*} \cdot (\mathbf{u} - \mathbf{u}^*), \tag{19}$$

   where $\nabla G^{\mathrm{T}}_{|\mathbf{u}^*} \equiv [\frac{\partial G}{\partial u_1}, \ldots, \frac{\partial G}{\partial u_n}]$ is the gradient vector of $G(\mathbf{u})$ at point $\mathbf{u}^*$.
4. The probability of failure is approximated by the probability content of the half-space $\beta - \boldsymbol{\alpha}^{\mathrm{T}}\mathbf{u} \leqslant 0$, where $\boldsymbol{\alpha} = -\frac{\nabla G_{|\mathbf{u}^*}}{\|\nabla G_{|\mathbf{u}^*}\|}$ is the outward unit vector normal to the limit state surface in $\mathbf{u}^*$ [47], and where β represents the minimum distance to the LSF. This leads to:

$$P_f \approx P_1 = \Phi(-\beta), \tag{20}$$

   where $\Phi(\cdot)$ is the CDF of the standard normal distribution.

Vector $\boldsymbol{\alpha}$ represents the sensitivities of the computed reliability to changes in the random variables $\mathbf{u}$. If the random variables $\mathbf{x}$ are not independent, however, vector $\boldsymbol{\alpha}$ is not informative in relation to the random variables $\mathbf{x}$. In that case, the sensitivity vector for the original variables $\mathbf{x}$ may be defined as [37]:

$$\boldsymbol{\gamma}^{\mathrm{T}} = \frac{\boldsymbol{\alpha}^{\mathrm{T}}\mathbf{J}_{\mathbf{u}^*,\mathbf{x}^*}\mathbf{D}'}{\|\boldsymbol{\alpha}^{\mathrm{T}}\mathbf{J}_{\mathbf{u}^*,\mathbf{x}^*}\mathbf{D}'\|}, \tag{21}$$

where $\mathbf{J}_{\mathbf{u}^*,\mathbf{x}^*}$ is the Jacobian of the transformation, and $\mathbf{D}'$ is the standard deviation matrix of equivalent normal variables $\mathbf{x}'$, defined as $\mathbf{x}' = \mathbf{x}^* + \mathbf{J}_{\mathbf{x}^*,\mathbf{u}^*}(\mathbf{u} - \mathbf{u}^*)$.

Vector $\boldsymbol{\gamma}$ also provides information that allows to differentiate between "load" and "resistance" variables [37]; if the ith component of vector $\boldsymbol{\gamma}$ is positive, that indicates the ith random variable is a "load" variable (i.e., a shift in the distribution toward higher values is associated to an increase in the probability of failure, and vice-versa). Similarly, a negative value of the ith component of $\boldsymbol{\gamma}$ indicates that the ith random variable is a "resistance" variable.

3.2. System reliability

A number of approximate and "exact" methods have been developed to solve the system reliability problem. Methods of interest in the context of rock engineering systems are discussed next.

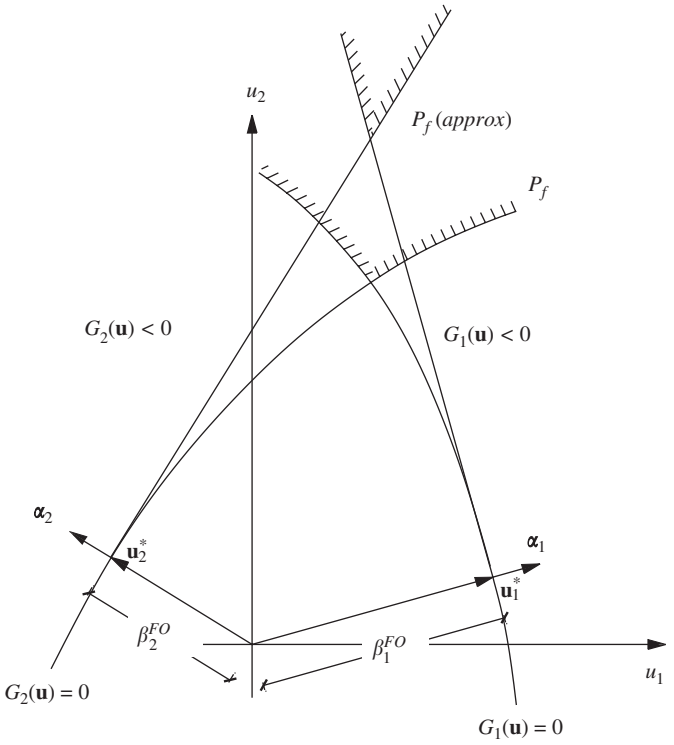

Fig. 6. First order approximation to probability of failure of parallel systems.

3.2.1. First order approximation of the probability of failure of parallel systems

The probability of failure of parallel system (i.e., cut-set) C_k may be estimated using the following polyhedral first order approximation of the failure domain (see Fig. 6) [39]:

$$P_f(C_k) \approx P\left(\bigcap_{i\in C_k} v_i \leqslant -\beta_i\right) = \Phi(-\boldsymbol{\beta}_{C_k}, \mathbf{R}), \tag{22}$$

where the $v_i \equiv \boldsymbol{\alpha}_i^T \mathbf{u}$ random variables have standard normal marginal distributions, and $\Phi(\boldsymbol{\beta}_{C_k}, \mathbf{R})$ is the CDF of the standard multinormal distribution evaluated at $-\boldsymbol{\beta}_{C_k}$, with correlation matrix, $\mathbf{R}$, given by $\mathbf{R}[i,j] = \boldsymbol{\alpha}_i^T \boldsymbol{\alpha}_j$. ($\boldsymbol{\beta}_{C_k}$ is a vector with the reliability indexes of each LSF in C_k, and $\boldsymbol{\alpha}_i$ and $\boldsymbol{\alpha}_j$ are the sensitivity vectors of the ith and jth LSF in C_k.)

3.2.2. System bounds to the probability of failure

An alternative approach is the use of reliability bounds. Several types of bounds have been proposed [39,48–50], using information about probabilities of single components or higher order joint probabilities. These bounds were, however, either limited to series systems, or were too wide to be of practical interest. Song and Der Kiureghian [38] have recently proposed new bounds for the reliability of general systems based on linear programming (LP). The strength of the LP bounds is that they have been shown to provide the narrowest possible bounds for any given information on component probabilities [38].

For a general system composed of N_g components the LP bounds may be obtained dividing the sample space of component events into 2^{N_g} mutually exclusive and collectively exhaustive (MECE) events e_i, with $i = 1, \ldots, 2^{N_g}$. Then, the probability of any general system may be expressed in terms of boolean operations of the probabilities of such MECE events. Calling $\mathbf{p} = (p_1, \ldots, p_{2^{N_g}})$, where p_i represents the probability of event e_i, the linear programming problem can be stated as [38]:

Optimize: (Minimize, maximize) the following objective function,

$$P(E_{\text{system}}) = \mathbf{c}^T \mathbf{p}, \tag{23}$$

where $\mathbf{c}$ represents the boolean vector of coefficients that define the probability of the system in terms of the probabilities of the MECE events.

Subject to constraints:

- Basic axioms of probability:

$$\sum_{i=1}^{2^{N_g}} p_i = 1, \tag{24}$$

$$p_i \geqslant 0 \quad \forall i,\ i = 1, \ldots, 2^{N_g}. \tag{25}$$

- Complete or incomplete probability information of component and joint probabilities. For instance, for complete information of uni- and bi-component probabilities, we would have:

$$P(E_i) \equiv P_i = \sum_{r:e_r \subseteq E_i} p_r, \tag{26}$$

$$P(E_j E_k) \equiv P_{j,k} = \sum_{r:e_r \subseteq E_j E_k} p_r, \tag{27}$$

where i represents those indices of individual components for which we have reliability information, and (j,k) represent those indices of component pairs for which we have bi-order joint reliability information.

3.2.3. Simulation methods

Simulation methods, such as Monte Carlo and directional simulation methods, are popular for reliability analysis of engineering systems. In the Monte Carlo simulation method, we define a boolean function $I(\mathbf{x})$ that represents the failure ($I(\mathbf{x}) = 1$) or safe ($I(\mathbf{x}) = 0$) state of the system for a set of values of the model's input random variables $\mathbf{x}$. That is, $I(\mathbf{x})$ is defined as:

$$I(\mathbf{x}) = \begin{cases} 1 & \text{if } \bigcup_{k=1}^{N_{CS}} \bigcap_{i\in C_k} g_i(\mathbf{x}) \leqslant 0, \\ 0 & \text{otherwise.} \end{cases} \tag{28}$$

Using a pseudo-random number generation algorithm [39], a sequence of N_s input vectors $\mathbf{x}_i$ is obtained, $(i = 1, \ldots, N_s)$, according to their joint statistical distribution. Then, the probability of failure of the system may be

estimated by:

$$P_f \approx \frac{1}{N_s}\sum_{i=1}^{N_s} I(\mathbf{x}_i). \quad (29)$$

In the case of the directional simulation method, we express vectors in the standard normal space as $\mathbf{u} = R\boldsymbol{\zeta}$, where $\boldsymbol{\zeta} = \mathbf{u}/\|\mathbf{u}\|$. Then, the probability of failure is given as the following conditional probability integral:

$$P_f = \int P\left[\left(\bigcup_{k=1}^{N_{CS}} \bigcap_{i\in C_k} G_i(R\boldsymbol{\zeta}) \leqslant 0\right) \middle| \boldsymbol{\zeta} = \mathbf{a}\right] \frac{f(\mathbf{a})}{h(\mathbf{a})} h(\mathbf{a})\,d\mathbf{a}, \quad (30)$$

where $f(\mathbf{a})$ represents the uniform distribution over the unit hyper-sphere, and $h(\mathbf{a})$ is a sampling density designed to improve the efficiency of the simulation, making those directions that more strongly affect the probability of failure to be sampled preferably [51].

The computation of the roots of the limit state functions in each direction $\mathbf{a}$ is needed to compute the probability of failure in Eq. (30). However, the problem of root finding is costly. For that reason, an approximate surface may be used to obtain solutions of the roots of $G_i(r_i\mathbf{a}) \equiv 0$, simplifying the computations required. In this paper, a first order approximation of the limit state functions was used. Accordingly, very similar solutions to those provided by the first order approximation given by Eq. (22) are obtained, as will be shown later.

3.3. Numerical implementation

In this work, we use CALREL [52] to perform simulation analyses and to perform the FORM analyses for component reliability that are needed to compute the first order approximation of the system reliability presented in Section 3.2.1. We implemented an efficient algorithm based on simulation with sequential conditional importance sampling (SCIS) [53] to compute $\Phi(\cdot,\cdot)$ in Eq. (22), given the information from the FORM analysis. Similarly, we implemented the LP bounds of the system reliability presented in Section 3.2.2 using commonly available programs for numerical analysis. Our implementation of the SCIS algorithm (using the GNU Scientific Library [54]) and of the LP method to compute the system reliability bounds (using MATLAB and R [55]) can be obtained from the authors upon request.

4. Example analyses

For the purpose of illustration of the type of results that can be obtained using the methodology, we use an example case based on the simple—yet commonly used—plane failure model presented in Section 2. However, the approach that we present in this paper is not limited to such simple problems. The system reliability framework analyses can be used to solve more complex problems by appropriate changes in the definition of the system and of the limit state functions. That is, the reliability approach can be employed as long as we can model the (deterministic) behavior of the components of the system in an adequate way first. CALREL is a generalized computer code that allows the use of limit state functions in the form of a set of user-defined subroutines or in the form of external codes [52], such as, for instance, finite element codes. Once that component reliabilities are computed and the system is defined, the first order approximation to the reliability of the system can be estimated independently of the complexity of the limit state functions involved. Similarly, LP bounds to problems with up to 17 components can be ordinarily solved on a PC [38]. Computers with larger memory or parallel computing may be necessary for larger problems [38].

4.1. Example case geometry and material properties

We assume that the overall slope geometry is deterministic with the location of the tension crack being the only random variable. Different slope heights, H, are considered, with H ranging from 10 to 40 m. The potential failure plane is inclined at 32° ($\psi_p = 32°$), and the angle of the slope cut is 60° ($\psi_f = 60°$). (An alternative model in which the potential failure surface is uncertain could be employed as well.) The specific weights of rock and water ($\gamma_{rock} = 25\,kN/m^3$ and $\gamma_w = 9.8\,kN/m^3$, respectively) are also considered deterministic.

Cohesion and friction angle along the failure surface are assumed to be random, as well as the position of the tension crack and the depth of water in the tension crack. Beta distribution is used to model friction angles between the different blocks, since it is very flexible and versatile; it is also bounded, avoiding problems that may arise when using unbounded distributions to model friction angles. Friction angles along block A, block B, and their contact surface are considered to have mean values of $\mu_{\phi_A} = 36°$, $\mu_{\phi_B} = 32°$ and $\mu_{\phi_{AB}} = 30°$, respectively. In all cases they are considered to be bounded at values equal to the mean plus or minus 10°. Cohesion values are chosen to be lognormally distributed, since the lognormal distribution is commonly used to model cohesion [29]. A mean value of $\mu_{c_A} = 20\,kPa$ is assigned for the cohesion along plane A, and $\mu_{c_B} = 18\,kPa$ is used for block B. In both cases the standard deviation of their distribution is assumed to be $\sigma_{c_A} = \sigma_{c_B} = 4\,kPa$. Finally, the passive force T acting at the toe of the slope is modeled using the normal distribution, with $\mu_T = 50\,kN$ and $\sigma_T = 3\,kN$.

The location of the tension crack and the percentage of the tension crack filled with water are modeled using dimensionless parameters ξ_{X_B} and ξ_{z_w}, respectively. The location of the tension crack follows a non-symmetric beta distribution, in order to represent the common observation that tension cracks are more commonly presented at the top of the slope [22]. It is also assumed that the drainage system of the slope prevents water levels from exceeding 50% of the crack height. Since no previous information on the distribution of ξ_{z_w} is known, the uniform distribution is

used to model the distribution of water level within the tension crack. Table 2 lists the statistical distributions used for each one of the random variables considered. Fig. 7 shows a graphical representation of their PDFs.

Further, the random variables are assumed to be correlated, with the correlation structure shown in Table 3. The location of the tension crack, the water level within the tension crack and the passive force at the toe of the slope (i.e., ξ_{X_B}, ξ_{z_w} and T, respectively) are considered to be independent of all the other variables, whereas shear strength parameters (i.e., friction angles and cohesion values) along the different joints are assumed to be correlated. Values of friction angle are assumed to be positively correlated, and a slight negative correlation is assumed between cohesion and friction to model the common observation in laboratory shear strength tests that cohesion and friction are not independent, with the cohesion dropping as the friction angle rises and vice-versa [56].

Table 2
Statistical distributions of input parameters in the slope stability model

Variable	Type	Parameters			
		p_1	p_2	p_3	p_4
ξ_{X_B}	Beta[a]	3.0	4.0	0.0	1.0
ξ_{z_w}	Uniform[b]	0.0	0.50		
ϕ_A (deg)	Beta[a]	5.0	5.0	26.0	46.0
ϕ_B (deg)	Beta[a]	5.0	5.0	22.0	42.0
ϕ_{AB} (deg)	Beta[a]	5.0	5.0	20.0	40.0
c_A (kPa)	Lognormal[c]	20.0	4.0		
c_B (kPa)	Lognormal[c]	18.0	4.0		
T (kN)	Normal[c]	50.0	3.0		

[a] $p_1 = q$, $p_2 = r$, $p_3 = a$, $p_4 = b$.
[b] $p_1 = a$, $p_2 = b$.
[c] $p_1 = \mu$, $p_2 = \sigma$.

Table 3
Correlation structure between random variables considered in the analysis

	ξ_{X_b}	ξ_{z_w}	ϕ_A	ϕ_B	ϕ_{AB}	c_A	c_B	T
ξ_{X_b}	1.0							
ξ_{z_w}	0.0	1.0			(Symmetric)			
ϕ_A	0.0	0.0	1.0					
ϕ_B	0.0	0.0	0.3	1.0				
ϕ_{AB}	0.0	0.0	0.3	0.3	1.0			
c_A	0.0	0.0	−0.1	0.0	0.0	1.0		
c_B	0.0	0.0	0.0	−0.1	0.0	0.3	1.0	
T	0.0	0.0	0.0	0.0	0.0	0.0	0.0	1.0

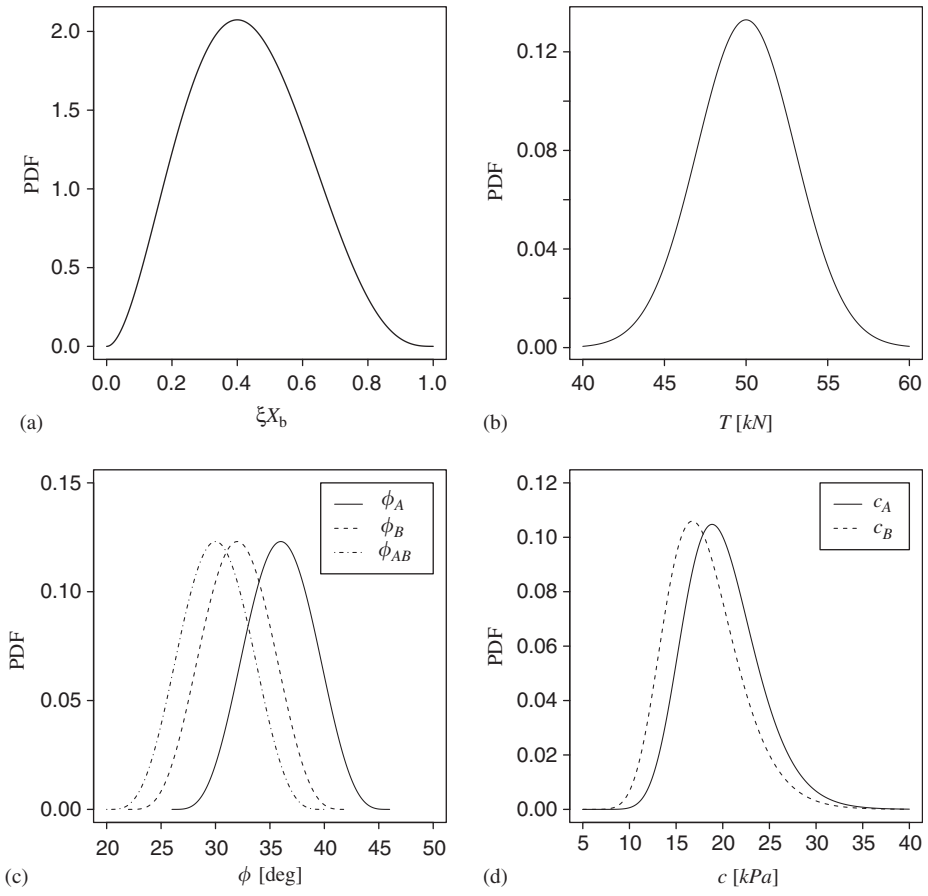

Fig. 7. Probability density functions of the random variables in the block stability model: (a) Tension crack location; (b) passive force at bottom of slope; (c) friction angles; (d) cohesion values.

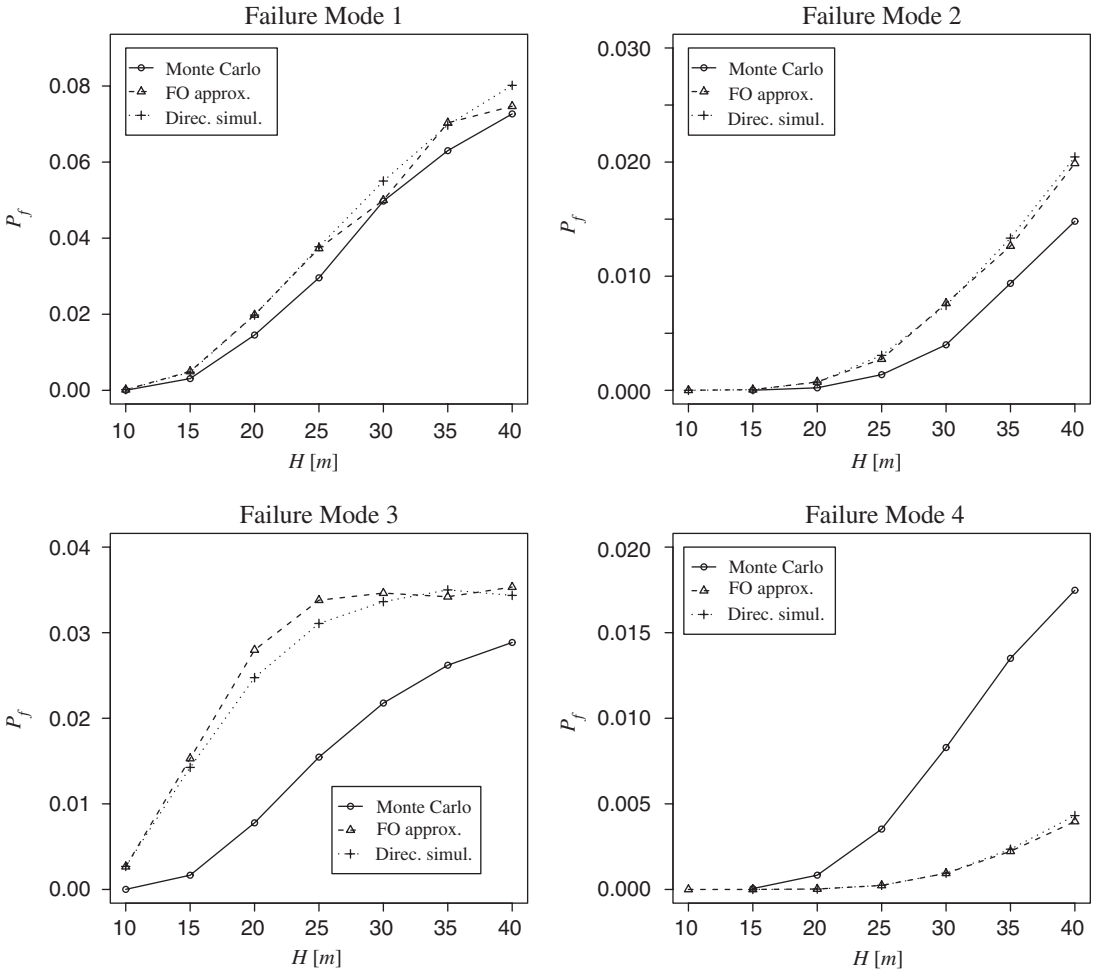

Fig. 8. Computed probability of failure for each cut-set (failure mode), using first order approximation and simulation methods.

4.2. Analysis results

CALREL was employed for FORM analyses of components in the example slope system. FORM results were then used to perform the polyhedral first order approximation of the failure domain presented in Section 3.2.1. The LP bounds presented in Section 3.2.2 were computed as well. CALREL was also used to perform first order directional simulation analyses, and to compute the "exact" reliability solution by means of Monte Carlo simulation. Fig. 8 shows the failure probabilities computed using these methods.

The contribution that each failure mode has in the overall probability of failure depends, among others, on the specific geometry of the slope, the distribution of locations of the tension crack, the distribution of water level conditions, and on the distribution of other forces acting on the blocks in each particular case. The ability to compute such contribution is a valuable feature of this methodology, since it provides quantitative information of interest in the design process that is not available otherwise. In this case, for instance, graphs in Fig. 8 show that Failure mode 1 (i.e., block A failing without interaction forces due to block B, with the tension crack being located at the top of the slope), and Failure mode 3 (i.e., block A failing without interaction forces due to block B, with the tension crack being located at face of the slope) have the highest probability of failure, while failure modes corresponding to cases in which there is interaction between blocks (i.e., Failure modes 2 and 4) are significantly less likely. Given this information, the stability of block A should be the primary concern when designing the slope, making the stability of block B of secondary importance. This may change, however, as we change some of the parameters over which the designer has control. For instance, if we increase the value of T (i.e., the passive force at the bottom of the slope), the stability of block A improves (therefore improving the reliability of the system), and failure modes with interaction between both blocks become more significant with respect to failure modes in which interaction does not occur.

Table 4 presents FORM results—computed for the case of $H = 20\,\text{m}$—for each limit state function controlling Failure mode 1. Such results include the computed design points, together with the sensitivity of the reliability solution to changes on the individual random variables

(the larger the absolute value of the ith component of $\boldsymbol{\gamma}$, the higher the sensitivity with respect to the ith random variable). Table 4 also shows the number of iterations of the iHL–RF algorithm before convergence, as well as computed values of the probability and reliability index for each limit state function.

In this case, the highest sensitivity corresponds to the location of the tension crack (represented by parameter ξ_{X_B}), suggesting that knowledge of the exact location of the tension crack is a key factor in the stability analysis, and hence emphasizing the importance of a good geological survey of discontinuities in the rock mass. Similarly, the sensitivity corresponding to the water level parameter ξ_{z_w} (i.e., the percentage of the tension crack that is filled with water; see Fig. 2) has a high positive value for limit state function $g_4(\mathbf{x})$, which models the stability of block A under Failure mode 1. Therefore, ξ_{z_w} corresponds to a "load" variable with respect to $g_4(\mathbf{x})$ (i.e., an increase in the value of ξ_{z_w} increases the probability of failure of the component and vice-versa). Similar results are obtained for the limit state function modeling the occurrence of no interaction forces between both blocks (i.e., $-g_2(\mathbf{x}) \leqslant 0$); accordingly, this shows that lowering the water level within the tension crack will reduce the probability of occurrence of Failure mode 1. However, this measure will also affect the probabilities of occurrence of other failure modes, and failure modes that were not as likely prior to the lowering of the water level might become more significant.

The discussion above illustrates the system nature of the problem; that is, mitigation of one potential mode of failure (by means of, for instance, increasing the support force T, or assuring an adequate drainage of the slope) changes the relative importance of the other failure modes. In this sense, it is the designer's duty to decide which slope design is preferable, based on probabilities, costs, consequences and the associated risks of the different modes of failure.

The sensitivities of the reliability results with respect to shear strength parameters depend on the selected limit state function. Table 4 shows that, for instance, the stability of block A in Failure mode 1 is quite sensitive to the values of cohesion and friction angle along its failure surface. As expected, both c_A and ϕ_A are found to be "resistance" variables, with the vector $\boldsymbol{\gamma}$ showing that ϕ_A is approximately twice more relevant than c_A in the safety of the slope. Similarly, the stability of block B (as given by limit state function $-g_2(\mathbf{x}) \leqslant 0$) is about twice more sensitive to changes in the friction angle, ϕ_B, than to changes in cohesion, c_B. Finally, the influence of changes in the value of the passive force at the toe of the slope, T, or in the angle of friction between both blocks, ϕ_{AB}, is not very significant in this case, suggesting that treating these two variables deterministically might be appropriate.

The results corresponding to simulation analyses of the probability of occurrence of Failure mode 1 for different values of H are presented in Table 5. The number of iterations needed by simulation methods is significantly higher than the number of iterations needed by the iHL–RF algorithm used in the FORM solution (see Table 4). This shows that the method based on first order approximation is computationally more efficient than traditional Monte Carlo-based solutions, which may be actually unachievable in some cases, specially when complex limit state functions are used or when dealing

Table 4
First order reliability results for components of Failure mode 1 ($H = 20$ m)

LSF	$g_1(\mathbf{x}) \leqslant 0$		$g_2(\mathbf{x}) \leqslant 0$		$g_4(\mathbf{x}) \leqslant 0$	
n_{iter}	3		179		16	
β^{FO}	−1.13		2.45		1.50	
P_f^{FO}	8.71×10^{-01}		7.11×10^{-03}		6.71×10^{-02}	
r.v.	$\mathbf{x}^*$	γ	$\mathbf{x}^*$	γ	$\mathbf{x}^*$	γ
ξ_{X_B}	0.64	−1.00	0.66	0.49	0.65	0.78
ξ_{z_w}	0.25	0.00	0.22	−0.06	0.40	0.55
ϕ_A	36.00	0.00	34.11	0.00	34.77	−0.27
ϕ_B	32.00	0.00	26.50	−0.77	31.61	0.00
ϕ_{AB}	30.00	0.00	28.11	0.00	29.61	0.00
c_A	19.61	0.00	18.45	0.00	18.95	−0.14
c_B	17.57	0.00	14.71	−0.40	17.32	0.00
T	50.00	0.00	50.00	0.00	49.97	−0.01

Table 5
Simulation results for Failure mode 1

H	Monte Carlo				Directional simulation			
	n_{iter}	P_f	β	cov(P_f)	n_{iter}	P_f	β	cov(P_f)
10	999000	2.10×10^{-05}	4.10	0.218	61500	1.65×10^{-04}	3.59	0.050
15	131000	3.08×10^{-03}	2.74	0.050	9700	4.76×10^{-03}	2.59	0.050
20	28000	1.45×10^{-02}	2.18	0.049	3800	1.98×10^{-02}	2.06	0.050
25	14000	2.96×10^{-02}	1.89	0.048	2300	3.77×10^{-02}	1.78	0.050
30	8000	4.98×10^{-02}	1.65	0.049	1700	5.50×10^{-02}	1.60	0.049
35	6000	6.30×10^{-02}	1.53	0.050	1400	6.97×10^{-02}	1.48	0.049
40	6000	7.27×10^{-02}	1.46	0.046	1300	8.02×10^{-02}	1.40	0.048

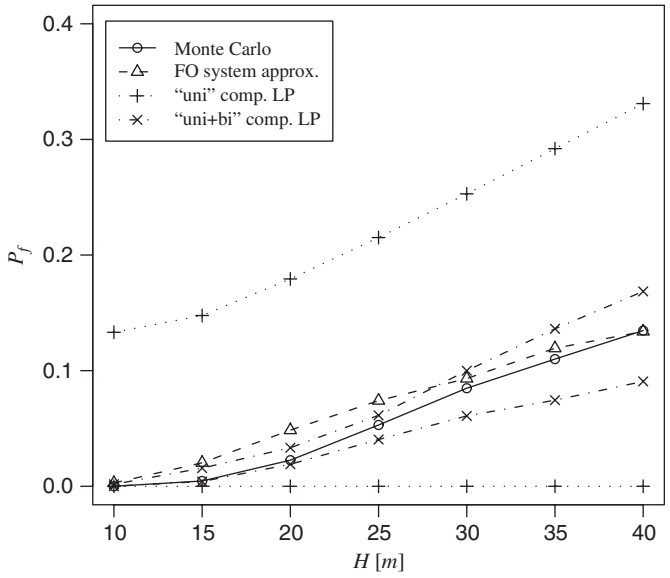

Fig. 9. Comparison of system probabilities obtained by different reliability methods.

with problems of low probability of failure, as we usually have in engineering practice.

Fig. 8 also shows that the method of estimation of probabilities based on first order approximation of the failure domain—even though more computationally efficient—is not particularly accurate in some cases. (The quality of the result will depend on the degree of non-linearity of the transformed limit state functions; see Fig. 6.) A fairly close agreement with the "exact" results provided by the Monte Carlo simulation method is obtained, however, when the contributions of each failure mode to the probability of failure of the complete system are added (see Fig. 9), since apparently over-predictions of the reliabilities of some failure modes balance out under-predictions of reliabilities of other failure modes.

The probability bounds for the complete slope system are also presented in Fig. 9. These results were obtained separately considering only uni-component failure probability information (i.e., $P(g_i(\mathbf{x})\leqslant 0)$, with $i=1,\ldots,N_g$), and both uni and joint bi-component failure probability information (i.e., $P(g_i(\mathbf{x})\leqslant 0\cap g_j(\mathbf{x})\leqslant 0)$, with $i=1,\ldots,N_g-1$ and $j=i+1,\ldots,N_g$). The results show that the probability bounds computed using information regarding probabilities of failure of individual components only are too wide to be of any practical interest. On the other hand, the probability bounds computed using both uni and joint bi-component failure information are much narrower, hence providing a greatly improved information on the reliability of the rock slope.

5. Conclusions

We present a reliability-based methodology for the analysis of rock slope stability problems based on a general systems approach. A disjoint cut-set formulation is used to compute the reliability of the system. Within that framework, each cut-set is associated with a failure mode and the probability of failure of the system is obtained as the sum of the probabilities of each failure mode. The results of an example analysis of a two-block sliding system show that, in this case, failure modes in which interaction between blocks does not occur (Failure modes 1 and 3) are significantly more likely than failure modes in which interaction occurs (Failure modes 2 and 4). The ability to quantify the relative importance of each failure mode is a valuable feature of the methodology that helps the designer to establish priorities during design and decision making.

The computed results also show that the method based on a first order approximation of the failure domain of parallel systems provides a simple and computationally efficient approach to perform reliability computations. FORM analyses employed with this method provide additional information of interest that is not easily obtained otherwise. In particular, the most likely failure conditions (i.e., design points) and the sensitivity of the reliability solution to changes in the random variables of the model can be computed, and "load" and "resistance" variables can be identified as well.

The use of simulation methods to solve the system reliability problem shows that the reliability results computed using the "exact" Monte Carlo method are obtained at the expense of a significantly higher computational cost when compared to first order approximations based on FORM. Similarly, it is shown that the method of first order directional simulation presents some computational advantages with respect to Monte Carlo method, providing results that are very similar to those given by the first order approximation of the probability of failure.

Finally, our results show that bounds of the probability of failure based on LP techniques provide accurate estimations of the system failure probability when information on both uni-component and joint bi-component probabilities is considered. The LP approach provides an interesting and flexible way of computing the range of possible failure probabilities for any given level of information. This method may also be used in conjunction with methods based on first order reliability approximations, so that we can use the information provided by FORM analyses—i.e., sensitivity measures, design points, etc.—at the same time that we have an estimation of the uncertainty associated to the first order results, given by the LP bounds.

Acknowledgments

Financial support for this research was provided by the Jane Lewis Fellowship from the University of California. The support of "Grupo de Investigaciones Medioambientales: Riesgos Geológicos e Ingeniería del Terreno" (RNM 221, PAI, Junta de Andalucía) of the University of Granada is gratefully acknowledged as well.

References

[1] Einstein HH. Risk and risk analysis in rock engineering. Tunnelling and Underground Space Technology 1996;11(2):141–55.

[2] Roberds WJ. Quantitative landslide risk assessment and management. In: Kuhne M, Einstein HH, Krauter E, Klapperich H, Pottler R, editors, Landslides—causes, impacts and countermeasures. Davos, Switzerland: Verlag Gluckauf; 2001. p. 585–95.

[3] Pine R, Roberds W. A risk-based approach for the design of rock slopes subject to multiple failure modes–illustrated by a case study in Hong Kong. Int J Rock Mech Min Sci 2005;42(2):261–75.

[4] Jiménez-Rodríguez R, Sitar N. Probabilistic identification of unstable blocks in rock excavations. In: der Kiureguian A, Madanat S, Pestana J, editors. Application of statistics and probability in civil engineering, vol. 2. Rotterdam: Millpress; 2003. p. 1301–8.

[5] Dershowitz WS, Einstein HH. Characterizing rock joint geometry with joint system models. Rock Mech Rock Eng 1988;21(1):21–51.

[6] Meyer T, Einstein HH. Geologic stochastic modeling and connectivity assessment of fracture systems in the Boston area. Rock Mech Rock Eng 2002;35(1):23–44.

[7] Kulatilake P, Fiedler R, Panda BB. Box fractal dimension as a measure of statistical homogeneity of jointed rock masses. Eng Geol 1997;48(3–4):217–29.

[8] La Pointe PR. Derivation of parent fracture population statistics from trace length measurements of fractal fracture populations. Int J Rock Mech Min Sci 2002;39:381–8.

[9] Young DS. Probabilistic slope analysis for structural failure. Int J Rock Mech Min Sci & Geomech Abstr 1993;30(7):1623–9.

[10] Starzec P, Andersson J. Application of two-level factorial design to sensitivity analysis of keyblock statistics from fracture geometry. Int J Rock Mech Min Sci 2002;39(2):243–55.

[11] Kuszmaul JS. Estimating keyblock sizes in underground excavations: accounting for joint set spacing. Int J Rock Mech and Min Sci 1999;36(2):217–32.

[12] Einstein HH. Modern developments in discontinuity analysis—the persistence-discontinuity problem. In: Hudson JA, editor, Comprehensive rock engineering, rock testing and site characterization, vol. 3, New York: Pergamon Press; 1993. p. 215–39.

[13] Mauldon M. Keyblock probabilities and size distributions—a first model for impersistent 2-d fractures. Int J Rock Mech Min Sci & Geomech Abstr 1995;32(6):575–83.

[14] Hoerger SF, Young DS. Probabilistic prediction of keyblock occurrences. In: Hustrulid WA, Johnson GA, editors, Rock mechanics; contributions and challenges; Proceedings of the 31st U.S. symposium. Rotterdam: A.A. Balkema; 1990. p. 229–36.

[15] Hoerger SF, Young DS. Probabilistic analysis of keyblock failures. In: Rossmanith HP, editor, Mechanics of jointed and faulted rock; Proceedings of the international conference. Rotterdam: A.A. Balkema; 1990. p. 503–8.

[16] Villaescusa E, Brown ET. Maximum likelihood estimation of joint size from trace length measurements. Rock Mech Rock Eng 1992; 25(2):67–87.

[17] Priest SD. The collection and analysis of discontinuity orientation data for engineering design, with examples. In: Hudson JA, editor, Comprehensive rock engineering; principles, practice & projects: rock testing and site characterization. Oxford: Pergamon Press; 1993. p. 167–92.

[18] Zhang LY, Einstein HH. Estimating the intensity of rock discontinuities. Int J Rock Mech Min Sci 2000;37(5):819–37.

[19] Zhang L, Einstein HH. Estimating the mean trace length of rock discontinuities. Rock Mech Rock Eng 1998;31(4):217–35.

[20] Song JJ, Lee CI. Estimation of joint length distribution using window sampling. Int J Rock Mech Min Sci 2001;38(4):519–28.

[21] Mauldon M. Estimating mean fracture trace length and density from observations in convex windows. Rock Mech Rock Eng 1998;31(4): 201–16.

[22] Hoek E, Bray J. Rock slope engineering. London: Institution of Mining and Metallurgy, 1981, rev. 3rd edition.

[23] Goodman RE. Introduction to rock mechanics. 2nd ed. New York: Wiley; 1989.

[24] Goodman RE, Shi G. Block theory and its application to rock engineering. Prentice-Hall international series in civil engineering and engineering mechanics. Englewood Cliffs, NJ: Prentice-Hall; 1985.

[25] Wittke W. Rock mechanics: theory and applications with case histories. Berlin, New York: Springer; 1990.

[26] Tamimi S, Amadei B, Frangopol DM. Monte Carlo simulation of rock slope stability. Comput Struct 1989;33(6):1495–505.

[27] Wang J, Tan W, Feng S, Zhou R. Reliability analysis of an open pit coal mine slope. Int J Rock Mech Min Sci & Geomech Abstr 2000; 37(4):715–21.

[28] Christian JT, Baecher GB. The point-estimate method with large numbers of variables. Int J Numer Anal Meth Geomech 2002;26(15): 1515–29.

[29] Duzgun HSB, Yucemen MS, Karpuz C. A methodology for reliability-based design of rock slopes. Rock Mech Rock Eng 2003; 36(2):95–120.

[30] Low BK. Reliability analysis of rock wedges. J Geotech Geoenviron Eng 1997;123(6):498–505.

[31] Low BK, Gilbert RB, Wright SG. Slope reliability analysis using generalized method of slices. J Geotech Geoenviron Eng 1998;124(4): 350–62.

[32] Hudson JA. Rock engineering systems: theory and practice. Ellis Horwood series in civil engineering. Geotechnics. New York: Ellis Horwood; 1992.

[33] Chowdhury RN, Xu DW. Geotechnical system reliability of slopes. Reliab Eng & System Safety 1995;47(3):141–51.

[34] Oka Y, Wu TH. System reliability of slope stability. J Geotech Eng 1990;116(8):1185–9.

[35] Goodman RE. Block theory and its application. Geotechnique 1995;45(3):383–422.

[36] Christian JT, Ladd CC, Baecher GB. Reliability applied to slope stability analysis. J Geotech Eng 1994;12(120):2180–207.

[37] Der Kiureghian A. Introduction to structural reliability, 1999. Class Notes for ''CE229—Structural Reliability''. Department of Civil Engineering, University of California, Berkeley.

[38] Song J, Der Kiureghian A. Bounds on system reliability by linear programming. J Eng Mech 2003;129(6):627–36.

[39] Ditlevsen O, Madsen H. Structural reliability methods. Chichester: Wiley; 1996.

[40] Ditlevsen O. Generalized second moment reliability index. J Struct Mech 1979;7(4):435–51.

[41] Bjerager P. On computation methods for structural reliability analysis. Structural Saf 1990;9:79–96.

[42] Der Kiureghian A, Liu P. Structural reliability under incomplete probability information. J Eng Mech 1986;1(112):85–104.

[43] Hohenbichler M, Rackwitz R. Non-normal dependent vectors in structural safety. J Eng Mech 1981;107(6):1227–38.

[44] Hasofer AM, Lind NC. An exact and invariant first-order reliability format. J Eng Mech 1974;100(1):111–21.

[45] Liu PL, Der Kiureghian A. Optimization algorithms for structural reliability. Struct Saf 1991;9:161–77.

[46] Zhang Y, Der Kiureghian A. Two improved algorithms for reliability analysis. In: Rackwithz R, Augusti G, Borri A, editors, Reliability and optimization of structural systems. Proceedings of the sixth IFIP WG 7.5 working conference on reliability and optimization of structural systems; 1994, 1995. p. 297–304.

[47] Bjerager P, Krenk S. Parametric sensitivity in first order reliability theory. J Eng Mech 1989;115(7):1577–82.

[48] Zhang YC. High-order reliability bounds for series systems and application to structural systems. Comput Struct 1993;46(2):381–6.

[49] Ditlevsen O. Narrow reliability bounds for structural systems. J Struct Mech 1979;7(4):453–72.

[50] Kounias EG. Bounds for the probability of a union, with applications. Ann Math Statist 1968;39(6):2154–8.

[51] Bjerager P. Probability integration by directional simulation. J Eng Mech 1988;114(8):1285–302.

[52] Liu PL, Lin HZ, Der Kiureghian A. CALREL user manual. Structural engineering, mechanics and materials. Department of Civil Engineering, University of California at Berkeley; 1989.
[53] Ambartzumian R, Der Kiureghian A, Ohanian V, Sukiasian H. Multinormal probability by sequential conditioned importance sampling: theory and application. Probab Eng Mech 1998;13(4):299–308.
[54] Galassi M, Davies J, Theiler J, Gough B, Jungman G, Booth M, Rossi F. GNU Scientific Library Reference Manual. 2nd ed. Network Theory Ltd.; 2003.
[55] R Development Core Team. R: A language and environment for statistical computing. R Foundation for Statistical Computing, Vienna, Austria, 2004. URL. http://www.R-project.org. ISBN 3-900051-00-3.
[56] Hoek E. Practical rock engineering. http://www.rocscience.com/hoek/PracticalRockEngineering.asp, 2000, World Wide Web edition.